93. B^0–$\overline{B}^0$ Mixing

Updated September 2017 by O. Schneider (Ecole Polytechnique Fédérale de Lausanne).

There are two neutral B^0–$\overline{B}^0$ meson systems, B^0_d–$\overline{B}^0_d$ and B^0_s–$\overline{B}^0_s$ (generically denoted B^0_q–$\overline{B}^0_q$, $q = s, d$), which exhibit particle-antiparticle mixing [1]. This mixing phenomenon is described in Ref. 2. In the following, we adopt the notation introduced in Ref. 2, and assume CPT conservation throughout. In each system, the light (L) and heavy (H) mass eigenstates,

$$|B_{\rm L,H}\rangle = p|B^0_q\rangle \pm q|\overline{B}^0_q\rangle\,, \tag{93.1}$$

have a mass difference $\Delta m_q = m_{\rm H} - m_{\rm L} > 0$, a total decay width difference $\Delta\Gamma_q = \Gamma_{\rm L} - \Gamma_{\rm H}$ and an average decay width $\Gamma_q = (\Gamma_{\rm L} + \Gamma_{\rm H})/2$. In the absence of CP violation in the mixing, $|q/p| = 1$, the differences are given by $\Delta m_q = 2|M_{12}|$ and $|\Delta\Gamma_q| = 2|\Gamma_{12}|$, where M_{12} and Γ_{12} are the off-diagonal elements of the mass and decay matrices [2]. The evolution of a pure $|B^0_q\rangle$ or $|\overline{B}^0_q\rangle$ state at $t = 0$ is given by

$$|B^0_q(t)\rangle = g_+(t)\,|B^0_q\rangle + \frac{q}{p}\,g_-(t)\,|\overline{B}^0_q\rangle\,, \tag{93.2}$$

$$|\overline{B}^0_q(t)\rangle = g_+(t)\,|\overline{B}^0_q\rangle + \frac{p}{q}g_-(t)\,|B^0_q\rangle\,, \tag{93.3}$$

which means that the flavor states remain unchanged (+) or oscillate into each other (−) with time-dependent probabilities proportional to

$$|g_\pm(t)|^2 = \frac{e^{-\Gamma_q t}}{2}\left[\cosh\left(\frac{\Delta\Gamma_q}{2}\,t\right) \pm \cos(\Delta m_q\,t)\right]\,, \tag{93.4}$$

where $\Gamma_q = (\Gamma_{\rm H} + \Gamma_{\rm L})/2$. In the absence of CP violation, the time-integrated mixing probability $\int |g_-(t)|^2\,dt/(\int |g_-(t)|^2\,dt + \int |g_+(t)|^2\,dt)$ is given by

$$\chi_q = \frac{x_q^2 + y_q^2}{2(x_q^2+1)}\,, \qquad \text{where} \qquad x_q = \frac{\Delta m_q}{\Gamma_q}\,, \qquad y_q = \frac{\Delta\Gamma_q}{2\Gamma_q}\,. \tag{93.5}$$

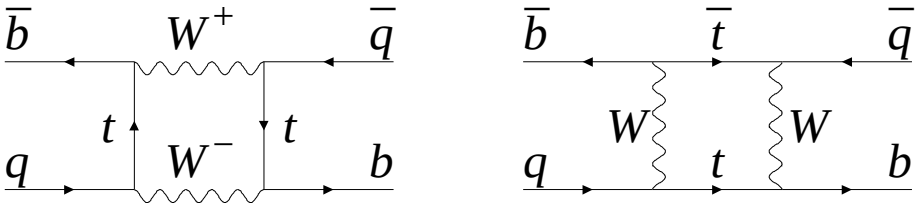

Figure 93.1: Dominant box diagrams for the $B^0_q \to \overline{B}^0_q$ transitions ($q = d$ or s). Similar diagrams exist where one or both t quarks are replaced with c or u quarks.

93.1. Standard Model predictions and phenomenology

In the Standard Model, the transitions $B^0_q \to \overline{B}^0_q$ and $\overline{B}^0_q \to B^0_q$ are due to the weak interaction. They are described, at the lowest order, by box diagrams involving two W bosons and two up-type quarks (see Fig. 93.1), as is the case for K^0–$\overline{K}^0$ mixing. However, the long range interactions arising from intermediate virtual states are negligible for the neutral B meson systems, because the large B mass is off the region of hadronic resonances. The calculation of the dispersive and absorptive parts of the box diagrams yields the following predictions for the off-diagonal element of the mass and decay matrices [3],

$$M_{12} = -\frac{G_F^2 m_W^2 \eta_B m_{B_q} B_{B_q} f_{B_q}^2}{12\pi^2}\, S_0(m_t^2/m_W^2)\,(V_{tq}^* V_{tb})^2\,, \tag{93.6}$$

$$\begin{aligned}\Gamma_{12} = {} & \frac{G_F^2 m_b^2 \eta'_B m_{B_q} B_{B_q} f_{B_q}^2}{8\pi} \\ & \times \left[(V_{tq}^* V_{tb})^2 + V_{tq}^* V_{tb} V_{cq}^* V_{cb}\, \mathcal{O}\!\left(\frac{m_c^2}{m_b^2}\right) \right. \\ & \left. + (V_{cq}^* V_{cb})^2\, \mathcal{O}\!\left(\frac{m_c^4}{m_b^4}\right) \right]\,, \end{aligned} \tag{93.7}$$

where G_F is the Fermi constant, m_W the W boson mass, and m_i the mass of quark i; m_{B_q}, f_{B_q} and B_{B_q} are the B^0_q mass, weak decay constant and bag parameter, respectively. The known function $S_0(x_t)$ can be approximated very well by $0.784\, x_t^{0.76}$ [4], and V_{ij} are the elements of the CKM matrix [5]. The QCD corrections η_B and η'_B are of order unity. The only non-negligible contributions to M_{12} are from box diagrams involving two top quarks. The phases of M_{12} and Γ_{12} satisfy

$$\phi_M - \phi_\Gamma = \pi + \mathcal{O}\left(\frac{m_c^2}{m_b^2}\right)\,, \tag{93.8}$$

implying that the mass eigenstates have mass and width differences of opposite signs. This means that, like in the K^0–$\overline{K}^0$ system, the heavy state is expected to have a smaller decay width than that of the light state: $\Gamma_{\rm H} < \Gamma_{\rm L}$. Hence, $\Delta\Gamma = \Gamma_{\rm L} - \Gamma_{\rm H}$ is expected to be positive in the Standard Model.

Furthermore, the quantity

$$\left|\frac{\Gamma_{12}}{M_{12}}\right| \simeq \frac{3\pi}{2}\frac{m_b^2}{m_W^2}\frac{1}{S_0(m_t^2/m_W^2)} \sim \mathcal{O}\left(\frac{m_b^2}{m_t^2}\right) \tag{93.9}$$

is small, and a power expansion of $|q/p|^2$ yields

$$\left|\frac{q}{p}\right|^2 = 1 + \left|\frac{\Gamma_{12}}{M_{12}}\right| \sin(\phi_M - \phi_\Gamma) + \mathcal{O}\left(\left|\frac{\Gamma_{12}}{M_{12}}\right|^2\right)\,. \tag{93.10}$$

Therefore, considering both Eqs. (93.8) and (93.9), the CP-violating parameter

$$1 - \left|\frac{q}{p}\right|^2 \simeq \mathrm{Im}\left(\frac{\Gamma_{12}}{M_{12}}\right) \tag{93.11}$$

is expected to be very small: $\sim \mathcal{O}(10^{-3})$ for the B^0_d–$\overline{B}^0_d$ system and $\lesssim \mathcal{O}(10^{-4})$ for the B^0_s–$\overline{B}^0_s$ system [6].

In the approximation of negligible CP violation in mixing, the ratio $\Delta\Gamma_q/\Delta m_q$ is equal to the small quantity $|\Gamma_{12}/M_{12}|$ of Eq. (93.9); it is hence independent of CKM matrix elements, *i.e.*, the same for the B^0_d–$\overline{B}^0_d$ and B^0_s–$\overline{B}^0_s$ systems. Calculations [7] yield $\sim 5 \times 10^{-3}$ with a $\sim 20\%$ uncertainty. Given the published experimental knowledge [8] on the mixing parameter x_q

$$\begin{cases} x_d = 0.770 \pm 0.004 & (B^0_d\text{–}\overline{B}^0_d \text{ system}) \\ x_s = 26.72 \pm 0.09 & (B^0_s\text{–}\overline{B}^0_s \text{ system}) \end{cases}, \tag{93.12}$$

the Standard Model thus predicts that $\Delta\Gamma_d/\Gamma_d$ is very small (below 1%), but $\Delta\Gamma_s/\Gamma_s$ considerably larger ($\sim 10\%$). These width differences are caused by the existence of final states to which both the B^0_q and $\overline{B}^0_q$ mesons can decay. Such decays involve $b \to c\overline{c}q$ quark-level transitions, which are Cabibbo-suppressed if $q = d$ and Cabibbo-allowed if $q = s$.

A complete set of Standard Model predictions for all mixing parameters in both the B^0_d–$\overline{B}^0_d$ and B^0_s–$\overline{B}^0_s$ systems can be found in Ref. 9.

93.2. Experimental issues and methods for oscillation analyses

Time-integrated measurements of B^0–$\overline{B}^0$ mixing were published for the first time in 1987 by UA1 [10] and ARGUS [11], and since then by many other experiments. These measurements are typically based on counting same-sign and opposite-sign lepton pairs from the semileptonic decay of the produced $b\overline{b}$ pairs. Such analyses cannot easily separate the contributions from the different b-hadron species, therefore, the clean environment of $\Upsilon(4S)$ machines (where only B^0_d and charged B_u mesons are produced) is in principle best suited to measure χ_d.

However, better sensitivity is obtained from time-dependent analyses aiming at the direct measurement of the oscillation frequencies Δm_d and Δm_s, from the proper time distributions of B^0_d or B^0_s candidates identified through their decay in (mostly) flavor-specific modes, and suitably tagged as mixed or unmixed. This is particularly true for the B^0_s–$\overline{B}^0_s$ system, where the large value of x_s implies maximal mixing, *i.e.*, $\chi_s \simeq 1/2$. In such analyses, the B^0_d or B^0_s mesons are either fully reconstructed, partially reconstructed from a charm meson, selected from a lepton with the characteristics of a $b \to \ell^-$ decay, or selected from a reconstructed displaced vertex. At high-energy colliders (LEP, SLC, Tevatron, LHC), the proper time $t = \dfrac{m_B}{p} L$ is measured from the distance L between the production vertex and the B decay vertex, and from an estimate of the B momentum p.

At asymmetric B factories (KEKB, PEP-II), producing $e^+e^- \to \Upsilon(4S) \to B^0_d\overline{B}^0_d$ events with a boost $\beta\gamma$ (= 0.425, 0.55), the proper time difference between the two B candidates is estimated as $\Delta t \simeq \dfrac{\Delta z}{\beta\gamma c}$, where Δz is the spatial separation between the two B decay vertices along the boost direction. In all cases, the good resolution needed on the vertex positions is obtained with silicon detectors.

The average statistical significance $\mathcal{S}$ of a B^0_q oscillation signal can be approximated as [12]

$$\mathcal{S} \approx \sqrt{N/2}\, f_{\rm sig}\, (1-2\eta)\, e^{-(\Delta m_q\, \sigma_t)^2/2}\,, \tag{93.13}$$

where N is the number of selected and tagged candidates, $f_{\rm sig}$ is the fraction of signal in that sample, η is the total mistag probability, and σ_t is the resolution on proper time (or proper time difference). The quantity $\mathcal{S}$ decreases very quickly as Δm_q increases; this dependence is controlled by σ_t, which is therefore a critical parameter for Δm_s analyses. At high-energy colliders, the proper time resolution $\sigma_t \sim \dfrac{m_B}{\langle p\rangle}\sigma_L \oplus t\dfrac{\sigma_p}{p}$ includes a constant contribution due to the decay length resolution σ_L (typically 0.04–0.3 ps), and a term due to the relative momentum resolution σ_p/p (typically 10–20% for partially reconstructed decays), which increases with proper time. At B factories, the boost of the B mesons is estimated from the known beam energies, and the term due to the spatial resolution dominates (typically 1–1.5 ps because of the much smaller B boost).

In order to tag a B^0_q candidate as mixed or unmixed, it is necessary to determine its flavor both in the initial state and in the final state. The initial and final state mistag probabilities, η_i and η_f, degrade $\mathcal{S}$ by a total factor $(1-2\eta) = (1-2\eta_i)(1-2\eta_f)$. In lepton-based analyses, the final state is tagged by the charge of the lepton from $b \to \ell^-$ decays; the largest contribution to η_f is then due to $\overline{b} \to \overline{c} \to \ell^-$ decays. Alternatively, the charge of a reconstructed charm meson (D^{*-} from B^0_d or D^-_s from B^0_s), or that of a kaon hypothesized to come from a $b \to c \to s$ decay [13], can be used. For fully-inclusive analyses based on topological vertexing, final-state tagging techniques include jet-charge [14] and charge-dipole [15,16] methods. At high-energy colliders, the methods to tag the initial state (*i.e.*, the state at production), can be divided into two groups: the ones that tag the initial charge of the $\overline{b}$ quark contained in the B^0_q candidate itself (same-side tag), and the ones that tag the initial charge of the other b quark produced in the event (opposite-side tag). On the same side, the sign of a charged pion, kaon or proton from the primary vertex is correlated with the production state of the B^0_q meson if that particle is a decay product of a B^{**} state or the first in the fragmentation chain [17,18]. Jet- and vertex-charge techniques work on both sides and on the opposite side, respectively. Finally, the charge of a lepton from $b \to \ell^-$, of a kaon from $b \to c \to s$ or of a charm hadron from $b \to c$ [19] can be used as an opposite-side tag, keeping in mind that its performance is degraded due to integrated mixing. At SLC, the beam polarization produced a sizeable forward-backward asymmetry in the $Z \to b\overline{b}$ decays, and provided another very interesting and effective initial state tag based on the polar angle of the B^0_q candidate [15]. Initial state tags have also been combined to reach $\eta_i \sim 26\%$ at LEP [18,20] or 22% at SLD [15] with full efficiency. In the case $\eta_f = 0$, this corresponds to an effective tagging efficiency $Q = \epsilon D^2 = \epsilon(1-2\eta)^2$, where ϵ is the tagging efficiency,

in the range $23-31\%$. The equivalent figure achieved by CDF during Tevatron Run I was $\sim 3.5\%$ [21], reflecting the fact that tagging is more difficult at hadron colliders. The CDF and DØ analyses of Tevatron Run II data reached $\epsilon D^2 = (1.8 \pm 0.1)\%$ [22] and $(2.5 \pm 0.2)\%$ [23] for opposite-side tagging, while same-side kaon tagging (for B_s^0 analyses) contributed an additional $3.7-4.8\%$ at CDF [22], and pushed the combined performance to $(4.7 \pm 0.5)\%$ at DØ [24]. LHCb, operating in the forward region at the LHC where the environment is different in terms of track multiplicity and b-hadron production kinematics, has reported $\epsilon D^2 = (2.10 \pm 0.25)\%$ [25] for opposite-side tagging, $(1.80 \pm 0.26)\%$ [26] for same-side kaon tagging, and $(2.11 \pm 0.11)\%$ [27] for same-side pion and proton tagging: the combined figure ranges typically between $(3.73 \pm 0.15)\%$ [28] and $(5.33 \pm 0.25)\%$ [29] depending on the mode in which the tagged B_s^0 meson is reconstructed, and reaches up to $(8.1 \pm 0.6)\%$ [30] for hadronic B_d^0 modes.

At B factories, the flavor of a B_d^0 meson at production cannot be determined, since the two neutral B mesons produced in a $\Upsilon(4S)$ decay evolve in a coherent P-wave state where they keep opposite flavors at any time. However, as soon as one of them decays, the other follows a time-evolution given by Eqs. (93.2) or (93.3), where t is replaced with Δt (which will take negative values half of the time). Hence, the "initial state" tag of a B can be taken as the final-state tag of the other B. Effective tagging efficiencies of 30% are achieved by BaBar and Belle [31], using different techniques including $b \to \ell^-$ and $b \to c \to s$ tags. It is worth noting that, in this case, mixing of the other B (*i.e.*, the coherent mixing occurring before the first B decay) does not contribute to the mistag probability.

Before the experimental observation of a decay-width difference, oscillation analyses typically neglected $\Delta\Gamma_q$ in Eq. (93.4), and described the time dependence with the functions $\Gamma_q e^{-\Gamma_q t}(1 \pm \cos(\Delta m_q t))/2$ (high-energy colliders) or $\Gamma_d e^{-\Gamma_d|\Delta t|}(1 \pm \cos(\Delta m_d \Delta t))/4$ (asymmetric $\Upsilon(4S)$ machines). As can be seen from Eq. (93.4), a non-zero value of $\Delta\Gamma_q$ would effectively reduce the oscillation amplitude with a small time-dependent factor that would be very difficult to distinguish from time resolution effects. Measurements of Δm_q are usually extracted from the data using a maximum likelihood fit.

93.3. Δm_d and $\Delta\Gamma_d$ measurements

Many B_d^0–$\overline{B}_d^0$ oscillations analyses have been published [32] by the ALEPH [33], DELPHI [16,34], L3 [35], OPAL [36,37] BaBar [38], Belle [39], CDF [17], DØ [23], and LHCb [40–43] collaborations. Although a variety of different techniques have been used, the individual Δm_d results obtained at LEP and Tevatron have remarkably similar precision. Their average is compatible with the recent and more precise measurements from the asymmetric B factories and the LHC. The systematic uncertainties are not negligible; they are often dominated by sample composition, mistag probability, or b-hadron lifetime contributions. Before being combined, the measurements are adjusted on the basis of a common set of input values, including the b-hadron lifetimes and fractions published in this *Review*. Some measurements are statistically correlated. Systematic correlations arise both from common physics sources (fragmentation

fractions, lifetimes, branching ratios of b hadrons), and from purely experimental or algorithmic effects (efficiency, resolution, tagging, background description). Combining all measurements [16,17,23,33–43] and accounting for all identified correlations yields $\Delta m_d = 0.5065 \pm 0.0016(\text{stat}) \pm 0.0011(\text{syst})$ ps^{-1} [8], a result dominated by the latest LHCb measurement with $B^0 \to D^{(*)-}\mu^+\nu_\mu X$ decays [43].

On the other hand, ARGUS and CLEO have published time-integrated measurements [44–46], which average to $\chi_d = 0.182 \pm 0.015$. Following Ref. 46, the width difference $\Delta\Gamma_d$ could in principle be extracted from the measured value of Γ_d and the above averages for Δm_d and χ_d (see Eq. (93.5)), provided that $\Delta\Gamma_d$ has a negligible impact on the Δm_d measurements. However, direct time-dependent studies published by DELPHI [16], BaBar [47], Belle [48], LHCb [49] and ATLAS [50] provide stronger constraints, which can be combined to yield [8]

$$\Delta\Gamma_d/\Gamma_d = -0.002 \pm 0.010\,. \tag{93.14}$$

Assuming $\Delta\Gamma_d = 0$ and no CP violation in mixing, and using the measured B^0_d lifetime of 1.520 ± 0.004 ps, the Δm_d and χ_d results are combined to yield the world average

$$\Delta m_d = 0.5064 \pm 0.0019 \text{ ps}^{-1} \tag{93.15}$$

or, equivalently,

$$\chi_d = 0.1860 \pm 0.0011\,. \tag{93.16}$$

This Δm_d value provides an estimate of $2|M_{12}|$, and can be used with Eq. (93.6) to extract $|V_{td}|$ within the Standard Model [51]. The main experimental uncertainties on the result come from m_t and Δm_d, but are still completely negligible with respect to the uncertainty due to the hadronic matrix element $f_{B_d}\sqrt{B_{B_d}} = 225 \pm 9$ MeV [52] obtained from recent three-flavor lattice QCD calculations.

93.4. Δm_s and $\Delta\Gamma_s$ measurements

After many years of intense search at LEP and SLC, B^0_s–$\overline{B}^0_s$ oscillations were first observed in 2006 by CDF using 1 fb^{-1} of Tevatron Run II data [22]. More recently LHCb observed B^0_s–$\overline{B}^0_s$ oscillations independently with $B^0_s \to D^-_s\pi^+$ [40,53], $B^0_s \to D^-_s\mu^+\nu$X [42] and even $B^0_s \to J/\psi K^+K^-$ [28] decays, using between 1 and 3 fb^{-1} of data collected at the LHC until the end of 2012. Taking systematic correlations into account, the average of all published measurements of Δm_s [22,28,40,42,53] is

$$\Delta m_s = 17.757 \pm 0.020(\text{stat}) \pm 0.007(\text{syst}) \text{ ps}^{-1}\,, \tag{93.17}$$

dominated by LHCb (see Fig. 93.2) and still statistically limited.

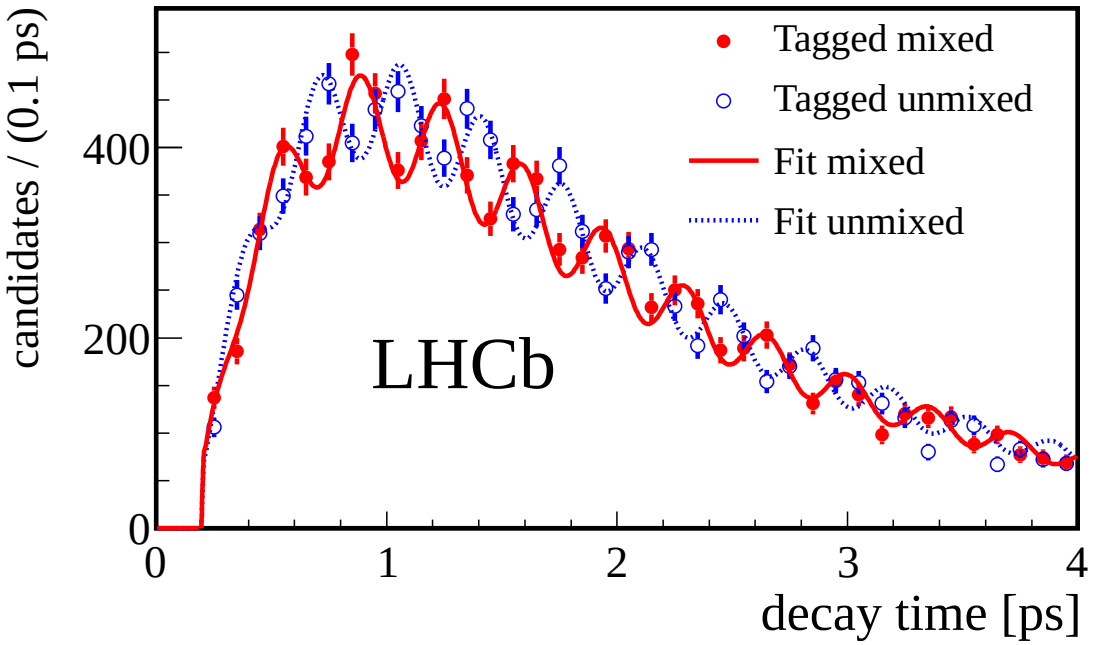

Figure 93.2: Proper time distribution of $B_s^0 \to D_s^- \pi^+$ candidates tagged as mixed (red) or unmixed (blue) in the LHCb experiment, displaying B_s^0–$\overline{B}_s^0$ oscillations (from Ref. 53).

The information on $|V_{ts}|$ obtained in the framework of the Standard Model is hampered by the hadronic uncertainty, as in the B_d^0 case. However, several uncertainties cancel in the frequency ratio

$$\frac{\Delta m_s}{\Delta m_d} = \frac{m_{B_s}}{m_{B_d}} \xi^2 \left| \frac{V_{ts}}{V_{td}} \right|^2 , \tag{93.18}$$

where $\xi = (f_{B_s}\sqrt{B_{B_s}})/(f_{B_d}\sqrt{B_{B_d}}) = 1.206 \pm 0.017$ is an SU(3) flavor-symmetry breaking factor obtained from recent three-flavor lattice QCD calculations [52]. Using the measurements of Eqs. (93.15) and (93.17), one can extract

$$\left| \frac{V_{td}}{V_{ts}} \right| = 0.2053 \pm 0.0004(\text{exp}) \pm 0.0029(\text{lattice}) , \tag{93.19}$$

in good agreement with (but much more precise than) the value obtained from the ratio of the $b \to d\gamma$ and $b \to s\gamma$ transition rates observed at the B factories [51].

The CKM matrix can be constrained using experimental results on observables such as Δm_d, Δm_s, $|V_{ub}/V_{cb}|$, ϵ_K, and $\sin(2\beta)$ together with theoretical inputs and unitarity conditions [51,54,55]. The constraint from our knowledge on the ratio $\Delta m_s/\Delta m_d$ is more effective in limiting the position of the apex of the CKM unitarity triangle than the one obtained from the Δm_d measurements alone, due to the reduced hadronic uncertainty in Eq. (93.18). We also note that the measured value of Δm_s is consistent with the

Standard Model prediction obtained from CKM fits where no experimental information on Δm_s is used, *e.g.*, 17.69 ± 0.93 ps^{-1} [54] or $16.89\,^{+0.47}_{-0.53}$ ps^{-1} [55].

Information on $\Delta\Gamma_s$ can be obtained from the study of the proper time distribution of untagged B_s^0 samples [56]. In the case of an inclusive B_s^0 selection [57], or a flavor-specific (semileptonic or hadronic) B_s^0 decay selection [20,58–60], both the short- and long-lived components are present, and the proper time distribution is a superposition of two exponentials with decay constants $\Gamma_{\rm L,H} = \Gamma_s \pm \Delta\Gamma_s/2$. In principle, this provides sensitivity to both Γ_s and $(\Delta\Gamma_s/\Gamma_s)^2$. Ignoring $\Delta\Gamma_s$ and fitting for a single exponential leads to an estimate of $1/\Gamma_s$ (called effective lifetime) with a relative bias proportional to $(\Delta\Gamma_s/\Gamma_s)^2$. An alternative approach, which is directly sensitive to first order in $\Delta\Gamma_s/\Gamma_s$, is to determine the effective lifetime of untagged B_s^0 candidates decaying to pure CP eigenstates; measurements exist for $B_s^0 \to D_s^+ D_s^-$ [59], $B_s^0 \to K^+K^-$ [60,61], $B_s^0 \to J/\psi\eta$ [62], $B_s^0 \to J/\psi f_0(980)$ [63], $B_s^0 \to J/\psi\pi^+\pi^-$ [64] and $B_s^0 \to J/\psi K_{\rm S}^0$ [65]. The extraction of $1/\Gamma_s$ and $\Delta\Gamma_s$ from such measurements, discussed in detail in Ref. 66, requires additional information in the form of theoretical assumptions or external inputs on weak phases and hadronic parameters. In what follows, we only use the effective lifetimes of decays to CP-even ($D_s^+ D_s^-$, $J/\psi\eta$) and CP-odd ($J/\psi f_0(980)$, $J/\psi\pi^+\pi^-$) final states where CP conservation can be assumed.

The best sensitivity to $1/\Gamma_s$ and $\Delta\Gamma_s$ is achieved by the time-dependent measurements of the $B_s^0 \to J/\psi K^+K^-$ (including $B_s^0 \to J/\psi\phi$) and $B_s^0 \to \psi(2S)\phi$ decay rates performed at CDF [67], DØ [68], ATLAS [69], CMS [70] and LHCb [28,71,72], where the CP-even and CP-odd amplitudes are separated statistically through a full angular analysis. The LHCb collaboration analyzes the $B_s^0 \to J/\psi K^+K^-$ decay considering that the K^+K^- system can be in a P-wave or S-wave state, and measures the dependence of the strong phase difference between the P-wave and S-wave amplitudes as a function of the K^+K^- invariant mass [28,73]; this allows the unambiguous determination of the sign of $\Delta\Gamma_s$, which is found to be positive. All these studies use both untagged and tagged B_s^0 candidates and are optimized for the measurement of the CP-violating phase $\phi_s^{c\bar{c}s}$, defined as the weak phase difference between the B_s^0–$\overline{B}_s^0$ mixing amplitude and the $b \to c\bar{c}s$ decay amplitude. As reported below in Eq. (93.28), the current experimental average of $\phi_s^{c\bar{c}s}$ is consistent with zero. Assuming no CP violation (*i.e.*, $\phi_s^{c\bar{c}s} = 0$) a combination [8] of the $B_s^0 \to J/\psi K^+K^-$, $J/\psi\phi$ and $\psi(2S)\phi$ analyses [28,67–72] and of effective lifetime measurements with flavor-specific [20,58–60] and pure CP [59,62–64] final states yields

$$\Delta\Gamma_s = +0.090 \pm 0.005 \text{ ps}^{-1} \quad \text{and} \quad 1/\Gamma_s = 1.509 \pm 0.004 \text{ ps}\,, \tag{93.20}$$

or, equivalently,

$$1/\Gamma_{\rm L} = 1.414 \pm 0.006 \text{ ps} \quad \text{and} \quad 1/\Gamma_{\rm H} = 1.619 \pm 0.009 \text{ ps}\,, \tag{93.21}$$

in good agreement with the Standard Model prediction $\Delta\Gamma_s = 0.088 \pm 0.020$ ps^{-1} [9].

Estimates of $\Delta\Gamma_s/\Gamma_s$ obtained from measurements of the $B_s^0 \to D_s^{(*)+} D_s^{(*)-}$ branching fractions are not included in the average, since they are based on the questionable [7] assumption that these decays account for all CP-even final states.

Table 93.1: $\overline{\chi}$ and b-hadron fractions (see text).

	in Z decays [8]	at Tevatron [8]	at LHC [85,87]
$\overline{\chi}$	0.1259 ± 0.0042	0.147 ± 0.011	
$f_u = f_d$	0.407 ± 0.007	0.344 ± 0.021	
f_s	0.101 ± 0.008	0.115 ± 0.013	
$f_{\rm baryon}$	0.084 ± 0.011	0.196 ± 0.046	
f_s/f_d	0.249 ± 0.023	0.333 ± 0.041	0.252 ± 0.012

93.5. Average *b*-hadron mixing probability and *b*-hadron production fractions at high energy

Mixing measurements can significantly improve our knowledge on the fractions f_u, f_d, f_s, and $f_{\rm baryon}$, defined as the fractions of B_u, B^0_d, B^0_s, and b-baryons in an unbiased sample of weakly decaying b hadrons produced in high-energy collisions. Indeed, time-integrated mixing analyses using lepton pairs from $b\overline{b}$ events at high energy measure the quantity

$$\overline{\chi} = f'_d\,\chi_d + f'_s\,\chi_s\,, \tag{93.22}$$

where f'_d and f'_s are the fractions of B^0_d and B^0_s hadrons in a sample of semileptonic b-hadron decays. Assuming that all b hadrons have the same semileptonic decay width implies $f'_q = f_q/(\Gamma_q \tau_b)$ $(q = s, d)$, where τ_b is the average b-hadron lifetime. Hence $\overline{\chi}$ measurements performed at LEP [74] and Tevatron [75,76], together with the χ_d average of Eq. (93.16) and the very good approximation $\chi_s = 1/2$ (in fact $\chi_s = 0.499308 \pm 0.000004$ from Eqs. (93.5), (93.17) and (93.20)), provide constraints on the fractions f_d and f_s.

The LEP experiments have measured $\mathcal{B}(\bar{b} \to B^0_s) \times \mathcal{B}(B^0_s \to D^-_s \ell^+ \nu_\ell X)$ [77], $\mathcal{B}(b \to \Lambda^0_b) \times \mathcal{B}(\Lambda^0_b \to \Lambda^+_c \ell^- \overline{\nu}_\ell X)$ [78], and $\mathcal{B}(b \to \Xi^-_b) \times \mathcal{B}(\Xi^-_b \to \Xi^- \ell^- \overline{\nu}_\ell X)$ [79] from partially reconstructed final states including a lepton, $f_{\rm baryon}$ from protons identified in b events [80], and the production rate of charged b hadrons [81]. The b-hadron fraction ratios measured at CDF are based on double semileptonic $K^*\mu\mu$ and $\phi\mu\mu$ final states [82] and lepton-charm final states [83]; in addition CDF and DØ have both measured strange b-baryon production [84]. On the other hand, fraction ratios have been studied by LHCb using fully reconstructed hadronic B^0_s and B^0_d decays [85], as well as semileptonic decays [86]. ATLAS has measured f_s/f_d using $B^0_s \to J/\psi\phi$ and $B^0 \to J/\psi K^{*0}$ decays [87]. Both CDF and LHCb observe that the ratio $f_{\Lambda^0_b}/(f_u + f_d)$ decreases with the transverse momentum of the lepton+charm system, indicating that the b-hadron fractions are not the same in different environments. We therefore provide sets of fractions separately for LEP and Tevatron (and no complete set for LHC, where strange b-baryon production has not been measured yet). A combination of all the available information under the constraints $f_u = f_d$, $f_u + f_d + f_s + f_{\rm baryon} = 1$, and Eq. (93.22), yields the averages shown in the first two columns of Table 93.1.

93.6. CP-violation studies

Evidence for CP violation in B^0_q–$\overline{B}^0_q$ mixing has been searched for, both with flavor-specific and inclusive B^0_q decays, in samples where the initial flavor state is tagged, usually with a lepton from the other b-hadron in the event. In the case of semileptonic (or other flavor-specific) decays, where the final-state tag is also available, the following asymmetry [2]

$$\mathcal{A}^q_{\rm SL} = \frac{N(\overline{B}^0_q(t) \to \ell^+\nu_\ell X) - N(B^0_q(t) \to \ell^-\overline{\nu}_\ell X)}{N(\overline{B}^0_q(t) \to \ell^+\nu_\ell X) + N(B^0_q(t) \to \ell^-\overline{\nu}_\ell X)} \simeq 1 - |q/p|^2_q \tag{93.23}$$

has been measured either in time-integrated analyses at CLEO [46,88], BaBar [89], CDF [90], DØ [91–93] and LHCb [94], or in time-dependent analyses at LEP [37,95], BaBar [47,96] and Belle [97]. In the inclusive case, also investigated at LEP [95,98], no final-state tag is used, and the asymmetry [99]

$$\frac{N(\overline{B}^0_q(t) \to \text{all}) - N(B^0_q(t) \to \text{all})}{N(\overline{B}^0_q(t) \to \text{all}) + N(B^0_q(t) \to \text{all})}$$

$$\simeq \mathcal{A}^q_{\rm SL}\left[\sin^2\left(\frac{\Delta m_q\, t}{2}\right) - \frac{x_q}{2}\sin(\Delta m_q\, t)\right] \tag{93.24}$$

must be measured as a function of the proper time to extract information on CP violation. In addition LHCb has studied the time dependence of the charge asymmetry of $B^0 \to D^{(*)-}\mu^+\nu_\mu X$ decays without tagging the initial state [100], which would be equal to

$$\frac{N(D^{(*)-}\mu^+\nu_\mu X) - N(D^{(*)+}\mu^-\bar{\nu}_\mu X)}{N(D^{(*)-}\mu^+\nu_\mu X) + N(D^{(*)+}\mu^-\bar{\nu}_\mu X)} = \mathcal{A}^d_{\rm SL}\frac{1-\cos(\Delta m_d\, t)}{2} \tag{93.25}$$

in absence of detection and production asymmetries.

The DØ collaboration measured a like-sign dimuon charge asymmetry in semileptonic b decays that deviates by $2.8\,\sigma$ from the tiny Standard Model prediction and concluded, from a more refined analysis in bins of muon impact parameters, that the overall discrepancy is at the level of $3.6\,\sigma$ [91]. In all other cases, asymmetries compatible with zero (and the Standard Model [9]) have been found, with a precision limited by the available statistics. Several of the analyses at high energy don't disentangle the B^0_d and B^0_s contributions, and either quote a mean asymmetry or a measurement of $\mathcal{A}^d_{\rm SL}$ assuming $\mathcal{A}^s_{\rm SL} = 0$: we no longer include these in the average. An exception is the dimuon DØ analysis [91], which separates the two contributions by exploiting their dependence on the muon impact parameter cut. The resulting measurements of $\mathcal{A}^d_{\rm SL}$ and $\mathcal{A}^s_{\rm SL}$ are then both compatible with the Standard Model. They are also correlated. We therefore perform a two-dimensional average of the measurements of Refs. [46,47,88,89,91–94,96,97,100] and obtain [8]

$$\mathcal{A}^d_{\rm SL} = -0.0021 \pm 0.0017\,, \text{ or } |q/p|_d = 1.0010 \pm 0.0008\,, \tag{93.26}$$

$$\mathcal{A}^s_{\rm SL} = -0.0006 \pm 0.0028\,, \text{ or } |q/p|_s = 1.0003 \pm 0.0014\,, \tag{93.27}$$

with a correlation coefficient of -0.054 between $\mathcal{A}^d_{\rm SL}$ and $\mathcal{A}^s_{\rm SL}$. These results show no evidence of CP violation and don't constrain yet the Standard Model.

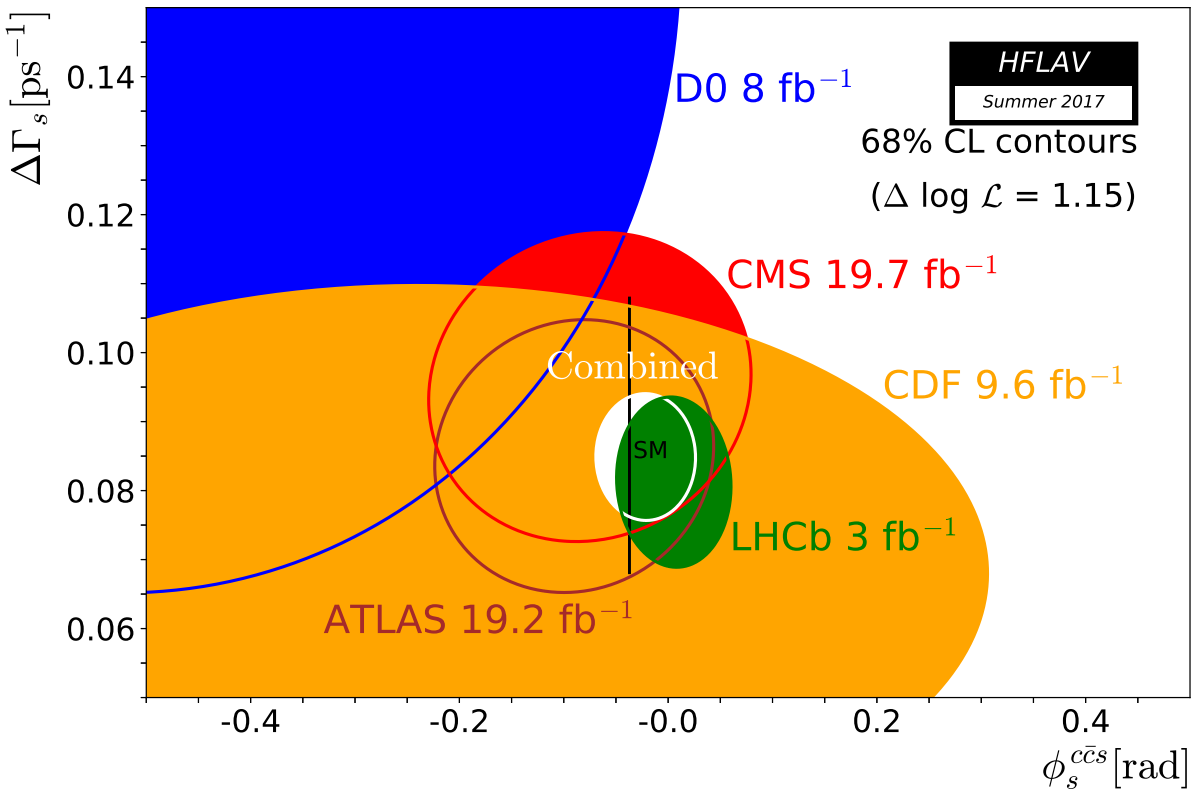

Figure 93.3: 68% CL contours in the $(\phi_s^{c\bar{c}s}, \Delta\Gamma_s)$ plane, showing the measurements from CDF [67], DØ [68], ATLAS [69], CMS [70] and LHCb [28,29,71,72,101], with their combination [8]. The thin black rectangle represents the Standard Model predictions of $\phi_s^{c\bar{c}s}$ [55] and $\Delta\Gamma_s$ [9].

CP violation induced by B_s^0–$\overline{B}_s^0$ mixing in $b \to c\bar{c}s$ decays has been a field of very active study in the past few years. In addition to the previously mentioned $B_s^0 \to J/\psi K^+K^-$ (including $B_s^0 \to J/\psi\phi$) and $B_s^0 \to \psi(2S)\phi$ studies, the decay modes $B_s^0 \to J/\psi\pi^+\pi^-$ (including $B_s^0 \to J/\psi f_0(980)$) [101] and $B_s^0 \to D_s^+ D_s^-$ [29] have also been analyzed by LHCb to measure $\phi_s^{c\bar{c}s}$, without the need for an angular analysis. The $J/\psi\pi^+\pi^-$ final state has been shown indeed to be (very close to) a pure CP-odd state [102]. A two-dimensional fit [8] of all these results [28,29,67–72,101] in the $(\phi_s^{c\bar{c}s}, \Delta\Gamma_s)$ plane, shown on Fig. 93.3, yields

$$\phi_s^{c\bar{c}s} = -0.021 \pm 0.031\,. \tag{93.28}$$

This is consistent with the Standard Model prediction for $\phi_s^{c\bar{c}s}$, which is equal to $-2\beta_s = -2\arg(-(V_{ts}V_{tb}^*)/(V_{cs}V_{cb}^*)) = -0.0370 \pm 0.0006$ [55], assuming negligible Penguin pollution.

93.7. Summary

B^0–$\overline{B}^0$ mixing has been and still is a field of intense study. The mass differences in the B^0_d–$\overline{B}^0_d$ and B^0_s–$\overline{B}^0_s$ systems are known to relative precisions of 0.38% and 0.12%, respectively. The non-zero decay width difference in the B^0_s–$\overline{B}^0_s$ system is well established, with a relative difference of $\Delta\Gamma_s/\Gamma_s = (13.5 \pm 0.8)\%$, meaning that the heavy state of the B^0_s–$\overline{B}^0_s$ system lives $\sim 14\%$ longer than the light state. In contrast, the relative decay width difference in the B^0_d–$\overline{B}^0_d$ system, $\Delta\Gamma_d/\Gamma_d = (-0.2 \pm 1.0)\%$, is still consistent with zero. CP violation in B^0_d–$\overline{B}^0_d$ or B^0_s–$\overline{B}^0_s$ mixing has not been observed yet, with precisions on the semileptonic asymmetries below 0.3%. CP violation induced by B^0_s–$\overline{B}^0_s$ mixing in $b \to c\bar{c}s$ transitions has not yet been observed either, with an uncertainty on the $\phi_s^{c\bar{c}s}$ phase of 31 mrad. Despite the recent improvements, all observations remain consistent with the Standard Model expectations.

However, the measurements where New Physics might show up are still statistically limited. More results are awaited from the LHC experiments and Belle II, with promising prospects for the investigation of the CP-violating phase $\arg(-M_{12}/\Gamma_{12})$ and an improved determination of $\phi_s^{c\bar{c}s}$.

Mixing studies have clearly reached the stage of precision measurements, where much effort is needed, both on the experimental and theoretical sides, in particular to further reduce the hadronic uncertainties of lattice QCD calculations. In the long term, a stringent check of the consistency of the B^0_d and B^0_s mixing amplitudes (magnitudes and phases) with all other measured flavor-physics observables will be possible within the Standard Model, leading to very tight limits on (or otherwise a long-awaited surprize about) New Physics.

References:

1. T.D. Lee and C.S. Wu, Ann. Rev. Nucl. Sci. **16**, 511 (1966); I.I. Bigi and A.I. Sanda, "CP violation," Cambridge Univ. Press, 2000; G.C. Branco, L. Lavoura, and J.P. Silva, "CP violation," Clarendon Press Oxford, 1999.
2. See the review on CP violation in the quark sector by T. Gershon and Y. Nir in this publication.
3. A.J. Buras, W. Slominski, and H. Steger, Nucl. Phys. **B245**, 369 (1984).
4. T. Inami and C.S. Lim, Prog. Theor. Phys. **65**, 297 (1981); for the power-like approximation, see A.J. Buras and R. Fleischer, page 91 in "Heavy Flavours II," eds. A.J. Buras and M. Lindner, Singapore World Scientific, 1998.
5. M. Kobayashi and K. Maskawa, Prog. Theor. Phys. **49**, 652 (1973).
6. I.I. Bigi *et al.*, in "CP violation," ed. C. Jarlskog, Singapore World Scientific, 1989.
7. A. Lenz and U. Nierste, `arXiv:1102.4274 [hep-ph]`; A. Lenz and U. Nierste, JHEP **06**, 072 (2007).
8. Y. Amhis *et al.* [HFLAV Group], "Averages of b-hadron, c-hadron, and τ-lepton properties as of summer 2016," `arXiv:1612.07233 [hep-ex]`, to appear in Eur. Phys. J. **C**; the combined results on b-hadron fractions, lifetimes and mixing parameters published in this *Review* have been obtained by the B oscillations working group of the Heavy Flavor Averaging (HFLAV)

Group, using the methods and procedures described in Chapter 3 of the above paper, after updating the list of inputs; for more information, see `http://www.slac.stanford.edu/xorg/hflav/osc/`.
9. T. Jubb, M. Kirk, A. Lenz, and G. Tetlalmatzi-Xolocotzi, Nucl. Phys. **B915**, 431 (2017); M. Artuso, G. Borissov, and A. Lenz, Rev. Mod. Phys. **88**, 045002 (2016).
10. C. Albajar *et al.* [UA1 Collab.], Phys. Lett. **B186**, 247 (1987).
11. H. Albrecht *et al.* [ARGUS Collab.], Phys. Lett. **B192**, 245 (1987).
12. H.-G. Moser and A. Roussarie, Nucl. Instrum. Methods **A384**, 491 (1997).
13. SLD Collab., SLAC-PUB-7228, SLAC-PUB-7229, and SLAC-PUB-7230, *28th Int. Conf. on High Energy Physics,* Warsaw, 1996; J. Wittlin, PhD thesis, SLAC-R-582, 2001.
14. ALEPH Collab., contrib. 596 to *Int. Europhysics Conf. on High Energy Physics,* Jerusalem, 1997.
15. K. Abe *et al.* [SLD Collab.], Phys. Rev. **D67**, 012006 (2003).
16. J. Abdallah *et al.* [DELPHI Collab.], Eur. Phys. J. **C28**, 155 (2003).
17. F. Abe *et al.* [CDF Collab.], Phys. Rev. Lett. **80**, 2057 (1998) and Phys. Rev. **D59**, 032001 (1999); Phys. Rev. **D60**, 051101 (1999); Phys. Rev. **D60**, 072003 (1999); T. Affolder *et al.* [CDF Collab.], Phys. Rev. **D60**, 112004 (1999).
18. R. Barate *et al.* [ALEPH Collab.], Eur. Phys. J. **C4**, 367 (1998); Eur. Phys. J. **C7**, 553 (1999).
19. R. Aaij *et al.* [LHCb Collab.], JINST **10**, P10005 (2015).
20. P. Abreu *et al.* [DELPHI Collab.], Eur. Phys. J. **C16**, 555 (2000).
21. See tagging summary on page 160 of K. Anikeev *et al.*, "B physics at the Tevatron: Run II and beyond," FERMILAB-PUB-01/97, `hep-ph/0201071`, and references therein.
22. A. Abulencia *et al.* [CDF Collab.], Phys. Rev. Lett. **97**, 242003 (2006).
23. V.M. Abazov *et al.* [DØ Collab.], Phys. Rev. **D74**, 112002 (2006).
24. V.M. Abazov *et al.* [DØ Collab.], Phys. Rev. Lett. **101**, 241801 (2008).
25. R. Aaij *et al.* [LHCb Collab.], Eur. Phys. J. **C72**, 2022 (2012).
26. R. Aaij *et al.* [LHCb Collab.], JINST **11**, P05010 (2016).
27. R. Aaij *et al.* [LHCb Collab.], Eur. Phys. J. **C77**, 238 (2017).
28. R. Aaij *et al.* [LHCb Collab.], Phys. Rev. Lett. **114**, 041801 (2015).
29. R. Aaij *et al.* [LHCb Collab.], Phys. Rev. Lett. **113**, 211801 (2014).
30. R. Aaij *et al.* [LHCb Collab.], Phys. Rev. Lett. **117**, 261801 (2016).
31. B. Aubert *et al.* [BaBar Collab.], Phys. Rev. Lett. **94**, 161803 (2005); K.-F. Chen *et al.* [Belle Collab.], Phys. Rev. **D72**, 012004 (2005).
32. Throughout this document we omit references of results that have been replaced by new published measurements.
33. D. Buskulic *et al.* [ALEPH Collab.], Z. Phys. **C75**, 397 (1997).
34. P. Abreu *et al.* [DELPHI Collab.], Z. Phys. **C76**, 579 (1997).
35. M. Acciarri *et al.* [L3 Collab.], Eur. Phys. J. **C5**, 195 (1998).
36. G. Alexander *et al.* [OPAL Collab.], Z. Phys. **C72**, 377 (1996); K. Ackerstaff *et al.* [OPAL Collab.], Z. Phys. **C76**, 417 (1997); G. Abbiendi *et al.* [OPAL Collab.], Phys. Lett. **B493**, 266 (2000).

37. K. Ackerstaff *et al.* [OPAL Collab.], Z. Phys. **C76**, 401 (1997).
38. B. Aubert *et al.* [BaBar Collab.], Phys. Rev. Lett. **88**, 221802 (2002) and Phys. Rev. **D66**, 032003 (2002); Phys. Rev. Lett. **88**, 221803 (2002); Phys. Rev. **D67**, 072002 (2003); Phys. Rev. **D73**, 012004 (2006).
39. N.C. Hastings *et al.* [Belle Collab.], Phys. Rev. **D67**, 052004 (2003); Y. Zheng *et al.* [Belle Collab.], Phys. Rev. **D67**, 092004 (2003); K. Abe *et al.* [Belle Collab.], Phys. Rev. **D71**, 072003 (2005).
40. R. Aaij *et al.* [LHCb Collab.], Phys. Lett. **B709**, 177 (2012).
41. R. Aaij *et al.* [LHCb Collab.], Phys. Lett. **B719**, 318 (2013).
42. R. Aaij *et al.* [LHCb Collab.], Eur. Phys. J. **C73**, 2655 (2013).
43. R. Aaij *et al.* [LHCb Collab.], Eur. Phys. J. **C76**, 422 (2016).
44. H. Albrecht *et al.* [ARGUS Collab.], Z. Phys. **C55**, 357 (1992); Phys. Lett. **B324**, 249 (1994).
45. J. Bartelt *et al.* [CLEO Collab.], Phys. Rev. Lett. **71**, 1680 (1993).
46. B.H. Behrens *et al.* [CLEO Collab.], Phys. Lett. **B490**, 36 (2000).
47. B. Aubert *et al.* [BaBar Collab.], Phys. Rev. Lett. **92**, 181801 (2004) and Phys. Rev. **D70**, 012007 (2004).
48. T. Higuchi *et al.* [Belle Collab.], Phys. Rev. **D85**, 071105 (2012).
49. R. Aaij *et al.* [LHCb Collab.], JHEP **04**, 114 (2014).
50. M. Aaboud *et al.* [ATLAS Collab.], JHEP **06**, 081 (2016).
51. See the review on the CKM quark-mixing matrix by A. Ceccucci, Z. Ligeti, and Y. Sakai in this publication.
52. S. Aoki *et al.* [FLAG Working Group], Eur. Phys. J. **C77**, 112 (2017); updated results at `http://itpwiki.unibe.ch/flag/`, dominated by A. Bazavov *et al.* [Fermilab Lattice and MILC Collab.], Phys. Rev. **D93**, 113016 (2016).
53. R. Aaij *et al.* [LHCb Collab.], New J. Phys. **15**, 053021 (2013).
54. M. Bona *et al.* [UTfit Collab.], JHEP **10**, 081 (2006); updated results at `http://www.utfit.org/`.
55. J. Charles *et al.* [CKMfitter Group], Phys. Rev. **D91**, 073007 (2015); updated results at `http://ckmfitter.in2p3.fr/`.
56. K. Hartkorn and H.-G. Moser, Eur. Phys. J. **C8**, 381 (1999).
57. M. Acciarri *et al.* [L3 Collab.], Phys. Lett. **B438**, 417 (1998).
58. D. Buskulic *et al.* [ALEPH Collab.], Phys. Lett. **B377**, 205 (1996); K. Ackerstaff *et al.* [OPAL Collab.], Phys. Lett. **B426**, 161 (1998); F. Abe *et al.* [CDF Collab.], Phys. Rev. **D59**, 032004 (1999); V.M. Abazov *et al.* [DØ Collab.], Phys. Rev. Lett. **114**, 062001 (2015); T. Aaltonen *et al.* [CDF Collab.], Phys. Rev. Lett. **107**, 272001 (2011); R. Aaij *et al.* [LHCb Collab.], Phys. Rev. Lett. **113**, 172001 (2014); R. Aaij *et al.* [LHCb Collab.], Phys. Rev. Lett. **119**, 101801 (2017).
59. R. Aaij *et al.* [LHCb Collab.], Phys. Rev. Lett. **112**, 111802 (2014).
60. R. Aaij *et al.* [LHCb Collab.], Phys. Lett. **B736**, 446 (2014).
61. R. Aaij *et al.* [LHCb Collab.], Phys. Lett. **B707**, 349 (2012).
62. R. Aaij *et al.* [LHCb Collab.], Phys. Lett. **B762**, 484 (2016).
63. T. Aaltonen *et al.* [CDF Collab.], Phys. Rev. **D84**, 052012 (2011); V.M. Abazov *et al.* [DØ Collab.], Phys. Rev. **D94**, 012001 (2016).

64. R. Aaij *et al.* [LHCb Collab.], Phys. Rev. **D87**, 112010 (2013).
65. R. Aaij *et al.* [LHCb Collab.], Nucl. Phys. **B873**, 275 (2013).
66. R. Fleischer and R. Knegjens, Eur. Phys. J. **C71**, 1789 (2011).
67. T. Aaltonen *et al.* [CDF Collab.], Phys. Rev. Lett. **109**, 171802 (2012).
68. V.M. Abazov *et al.* [DØ Collab.], Phys. Rev. **D85**, 032006 (2012).
69. G. Aad *et al.* [ATLAS Collab.], Phys. Rev. **D90**, 052007 (2014); JHEP **08**, 147 (2016).
70. V. Khachatryan *et al.* [CMS Collab.], Phys. Lett. **B757**, 97 (2016).
71. R. Aaij *et al.* [LHCb Collab.], JHEP **08**, 037 (2017).
72. R. Aaij *et al.* [LHCb Collab.], Phys. Lett. **B762**, 253 (2016).
73. R. Aaij *et al.* [LHCb Collab.], Phys. Rev. Lett. **108**, 241801 (2012).
74. ALEPH, DELPHI, L3, OPAL, and SLD Collabs.; Physics Reports **427**, 257 (2006); we use the $\overline{\chi}$ average given in Eq. (5.39).
75. D. Acosta *et al.* [CDF Collab.], Phys. Rev. **D69**, 012002 (2004).
76. V.M. Abazov *et al.* [DØ Collab.], Phys. Rev. **D74**, 092001 (2006).
77. P. Abreu *et al.* [DELPHI Collab.], Phys. Lett. **B289**, 199 (1992); P.D. Acton *et al.* [OPAL Collab.], Phys. Lett. **B295**, 357 (1992); D. Buskulic *et al.* [ALEPH Collab.], Phys. Lett. **B361**, 221 (1995).
78. P. Abreu *et al.* [DELPHI Collab.], Z. Phys. **C68**, 375 (1995); R. Barate *et al.* [ALEPH Collab.], Eur. Phys. J. **C2**, 197 (1998).
79. D. Buskulic *et al.* [ALEPH Collab.], Phys. Lett. **B384**, 449 (1996); J. Abdallah *et al.* [DELPHI Collab.], Eur. Phys. J. **C44**, 299 (2005).
80. R. Barate *et al.* [ALEPH Collab.], Eur. Phys. J. **C5**, 205 (1998).
81. J. Abdallah *et al.* [DELPHI Collab.], Phys. Lett. **B576**, 29 (2003).
82. F. Abe *et al.* [CDF Collab.], Phys. Rev. **D60**, 092005 (1999).
83. T. Aaltonen *et al.* [CDF Collab.], Phys. Rev. **D77**, 072003 (2008); T. Affolder *et al.* [CDF Collab.], Phys. Rev. Lett. **84**, 1663 (2000); the measurement of $f_{\rm baryon}/f_d$ in the latter paper has been updated based on T. Aaltonen *et al.* [CDF Collab.], Phys. Rev. **D79**, 032001 (2009).
84. V.M. Abazov *et al.* [DØ Collab.], Phys. Rev. Lett. **99**, 052001 (2007); V.M. Abazov *et al.* [DØ Collab.], Phys. Rev. Lett. **101**, 232002 (2008); T. Aaltonen *et al.* [CDF Collab.], Phys. Rev. **D80**, 072003 (2009).
85. R. Aaij *et al.* [LHCb Collab.], JHEP **04**, 001 (2013); the LHCb average of f_s/f_d has been updated in LHCb Collab., LHCb-CONF-2013-011 (2013).
86. R. Aaij *et al.* [LHCb Collab.], Phys. Rev. **D85**, 032008 (2012).
87. G. Aad *et al.* [ATLAS Collab.], Phys. Rev. Lett. **115**, 262001 (2015).
88. D.E. Jaffe *et al.* [CLEO Collab.], Phys. Rev. Lett. **86**, 5000 (2001).
89. J.P. Lees *et al.* [BaBar Collab.], Phys. Rev. Lett. **114**, 081801 (2015).
90. F. Abe *et al.* [CDF Collab.], Phys. Rev. **D55**, 2546 (1997).
91. V.M. Abazov *et al.* [DØ Collab.], Phys. Rev. **D89**, 012002 (2014).
92. V.M. Abazov *et al.* [DØ Collab.], Phys. Rev. **D86**, 072009 (2012).
93. V.M. Abazov *et al.* [DØ Collab.], Phys. Rev. Lett. **110**, 011801 (2013).
94. R. Aaij *et al.* [LHCb Collab.], Phys. Rev. Lett. **117**, 061803 (2016).
95. R. Barate *et al.* [ALEPH Collab.], Eur. Phys. J. **C20**, 431 (2001).

96. J.P. Lees *et al.* [BaBar Collab.], Phys. Rev. Lett. **111**, 101802 (2013).
97. E. Nakano *et al.* [Belle Collab.], Phys. Rev. **D73**, 112002 (2006).
98. G. Abbiendi *et al.* [OPAL Collab.], Eur. Phys. J. **C12**, 609 (2000).
99. M. Beneke, G. Buchalla, and I. Dunietz, Phys. Lett. **B393**, 132 (1997); I. Dunietz, Eur. Phys. J. **C7**, 197 (1999).
100. R. Aaij *et al.* [LHCb Collab.], Phys. Rev. Lett. **114**, 041601 (2015).
101. R. Aaij *et al.* [LHCb Collab.], Phys. Lett. **B736**, 186 (2014).
102. R. Aaij *et al.* [LHCb Collab.], Phys. Rev. **D86**, 052006 (2012).